Application of electrical impedance tomography in diagnosis of emphysema—a clinical study

B Murat Eyüboğlu†, A Füsun Öner‡§, Uğur Baysal†, Çiğdem Biber‡, A İhsan Keyf‡, Ülkü Yılmaz‡ and Yurdanur Erdoğan‡

† Department of Electrical and Electronics Engineering, Hacettepe University, 06532 Beytepe, Ankara, Turkey
‡ Atatürk Chest Diseases and Surgery Center, Keçiören, Ankara, Turkey

Abstract. In this paper, electrical impedance tomography (EIT) ventilation images from a group of 12 patients (11 patients with emphysema and one patient with only chronic obstructive pulmonary disease (COPD) (chronic bronchitis)) and a group of 15 normal subjects were acquired using a Sheffield mark 1 EIT system, at the levels of second, fourth and sixth intercostal spaces. Patients were diagnosed based on CT scans of the thorax, pulmonary function tests and posteroanterior x-ray graphs. One of the patients with emphysema has also a malignant lung tumour. Ventilation-related conductivity changes at total lung capacity (TLC) relative to residual volume were measured quantitatively in EIT images. These quantitative values demonstrate marked differences compared to those values obtained from the EIT images of 15 normal subjects. The EIT images of the patients were also compared with the CT images.

In addition to the visual examination of the EIT images a statistical confidence test is applied to compare the images of the patients with the images of the normal subjects. Prior to statistical analysis all images are normalized with TLC to minimize the effect of mismatch between the TLC of different subjects. A normal mean image is created by averaging the normalized images from the normal subjects, at each intercostal space level. Than a 95% confidence interval is defined for each normal mean image. For each image of the patients, a confidence test image, which represents the deviations from the 95% confidence interval of the normal mean image, is created. The regions with emphysematous bulla and parencyhma are detectable in the confidence test images as regions of positive and negative deviations from the confidence interval of the normal mean, respectively. In the test images, it is possible to differentiate emphysematous parenchyma from emphysematous bulla, tumour structure, and COPD. However, the emphysematous bulla, the tumour structure, and COPD result in the same type of defect in the test images and are therefore indistinguishable from each other. In some cases, off-plane contributions in the EIT images may result in underestimation of the defects. EIT may be a useful screening device in detecting emphysema rather than a diagnostic tool.

1. Introduction

Electrical impedance tomography (EIT) images of the human thorax have been produced successfully, by several groups. These images represent the changes in conductivity of the lungs associated with pulmonary function, either in ventilation or in cardiac gated perfusion studies (Harris *et al* 1987, 1988, Eyüboğlu *et al* 1989, Holder and Temple 1993, Leathard *et al* 1994). Studies on the diagnosis of pulmonary oedema and pulmonary embolism were performed on a limited number of patients and EIT was shown to be promising in detection of these cardiopulmonary abnormalities (Harris *et al* 1987, McArdle *et al* 1988, Leathard *et al* 1994). Holder and Temple (1993) compared ventilation and perfusion EIT images of

§ On leave of absence at: Pulmonary and Critical Care Division, The University of Pennsylvania Hospital, Philadelphia, PA 19104-4283, USA.

four patients with lung disorders with images from 30 healthy volunteers and confirmed that significant changes in impedance can be related to both ventilation and perfusion. However, they noted that it seems unlikely to determine any precise anatomical location of the lesions in EIT images. In a study with 10 normal subjects and two patients, Leathard *et al* (1994) observed marked differences between the images obtained from the normal subjects and the patients with pulmonary emboli. Harris *et al* (1988) reported a consistently high correlation between the volume of air inspired and the magnitude of changes in the lung resistivity, on the normal subjects. Harris *et al* (1987) demonstrated, on one patient, that the resolution of electrical impedance imaging is sufficient to locate emphysema.

In this paper, results of a study on a group of 11 patients with diagnosed emphysema and one patient with chronic obstructive pulmonary disease (COPD) (chronic bronchitis) are presented. CT scans of the thorax, pulmonary function test (PFT) and posteroanterior x-ray graphs are also obtained from each patient, prior to the EIT study. Ventilation-related conductivity changes are measured quantitatively in the EIT images of these patients and 15 normal subjects with no known respiratory abnormality, at the second, fourth and sixth intercostal space levels. The images of the patients are compared with the mean of the EIT images obtained from the normal subjects. This comparison is done both by visual inspection and by applying a statistical confidence test to locate the deviations from the mean of the normal images.

2. Methods

2.1. Data acquisition on normal subjects

In the first part of this study, EIT ventilation scans are obtained from a group of 15 male subjects (age mean: 25, age range: 20–31, standard deviation: 3.6) with no known respiratory abnormalities. A 16-electrode Sheffield mark 1 EIT system is used (Brown and Seagar 1987). This system uses the adjacent electrode current drive at 50 kHz. A 17th electrode is placed on the left abdomen for common-mode feedback. All the electrodes are Ag–AgCl disposable ECG electrodes (Skintact diameter 55 mm adult). Skin is cleaned with alcohol prior to electrode attachment.

During the data acquisition, subjects are sitting up on a chair. On each subject, data are acquired successively, at second, fourth and, sixth intercostal spaces (on the midclavicular line). At each level, 16 electrodes are equally spaced around the thorax. A reference data set is collected initially at residual volume, after the subject has exhaled from vital capacity into a spirometer (Mijnhart Vicatest 3 dry spirometer). Subsequently, EIT scans are performed sequentially at several inspiratory manoeuvres, each followed by a breath hold, up to the vital capacity. Inspiration and breath hold are synchronized with data collection. All volumes are measured in litres at atmospheric pressure and temperature. This scenario is repeated at each of the three intercostal space levels.

The data collection rate is 10 data cycles per second. In one data cycle, current is applied successively between all adjacent pairs of electrodes and the potential differences measured between all the remaining adjacent electrodes. To improve the signal to noise ratio and to suppress the effect of cardiac-related impedance changes in the thorax, 20 data cycles acquired at the same inspiratory manoeuvre are averaged prior to image reconstruction.

2.2. Data acquisition on patients with emphysema

EIT ventilation scans were obtained from 12 male patients. In addition to the EIT images, CT scans of the thorax, PFT, and posteroanterior x-ray graphs of each patient were also

obtained. Based on their clinical history and conventional CT scans of the thorax, 11 of the patients were diagnosed with different levels of emphysema. One patient has only chronic bronchitis without emphysema. One of the 11 patients has a malignant tumour as well as regions with emphysematous bulla. EIT data acquisition details are the same as used for the group of normal subjects explained in section 2.1.

2.3. *Image reconstruction, segmentation, and analysis*

Filtered backprojection along equipotential lines (Barber and Seagar 1987) is used for image reconstruction. The images represent the distribution of percentage conductivity change between the reference data cycle and each of the subsequent scans performed during the breath hold period. The images are displayed in a colour scale with superimposed contour plots outlining the equal-conductivity change zones. The contours are labelled with corresponding values of percentage conductivity change.

   Although the images are acquired sequentially at several inspiratory manoeuvres, only the images acquired at total lung capacity (TLC) are utilized during the visual inspection and the statistical analysis of the images from the patients. Prior to the statistical analysis, all images are normalized with the volume of inspired air (i.e., TLC). Hence, each normalized image demonstrates the distribution of percentage change in conductivity per litre of inspired air. Normalizing with TLC should minimize the effect of the age and the lung capacity mismatch between the patients and the group of normals.

   For analysis, the images are divided into six segments as shown in figure 1. These segments are labelled as left anterior (LA), right anterior (RA), left interior (LI), right interior (RI), left posterior (LP), and right posterior (RP). The visual assessment of the colour scale images is subjective and hence may result in considerable interobserver and intraobserver variability. Image segmentation of figure 1 and the numerical contour labels are used to minimize interobserver and intraobserver variability in visual examination of the images.

Right Anterior	Left Anterior
Right Interior	Left Interior
Right Posterior	Left Posterior

Figure 1. Segmentation used for quantitative analysis of the images.

   For statistical analysis of the images, a normal mean image is created, at each intercostal space level, by averaging normalized images of 15 normal subjects. An image representing the standard deviation of each pixel's value in the corresponding normal mean image is also created. Based on these normal mean images and their corresponding standard deviations, a 95% confidence interval is defined for each pixel in an image. Then, a t test is applied to each normalized image of the patients (Hines and Montgomery 1990). In an image of a patient, if a pixel's value falls into the 95% confidence interval of the normal mean image,

then the corresponding pixel's value is set to zero. Otherwise, the pixel's value is considered as being significantly different from the normal and the pixel's value is set equal to

$$\mu_i - p_i$$

where μ_i is the ith pixel's value in the normal mean image and p_i is the ith pixel's value in the patient's image. The value $\mu_i - p_i$ shows the deviation from the mean. This way, the result of the confidence test can be displayed in the form of an image. This test image demonstrates the zones of deviation from the 95% confidence interval of the normal mean image.

3. Results of the study on the group of normal subjects

Our study on a group of normal subjects showed that the spatial resolution of the EIT system is sufficient to image the differences in the level of ventilation, in different segments of the lungs. In the sequential EIT images acquired at several inspiratory manoeuvres, a consistently linear relation between the volume of the air inspired and the impedance index of the lungs is observed in agreement with Harris *et al* (1988). Similar to the results reported by Harris *et al* (1987), at low inspiratory volumes an increase is observed in the region over which the conductivity change occurs. At higher inspiratory volumes, a higher decrease in the conductivity is observed.

The reconstructed images from the normal subjects represent the percentage changes in lung conductivity at TLC with respect to the conductivity distribution at residual volume. In these ventilation images, the regions filled with air following inspiration appear as regions of decreased conductivity. To analyse the images quantitatively, the image segmentation in figure 1 is used. The maximum percentage conductivity change for each image segment is determined at each intercostal level, from all the normal subjects. The mean and standard deviation of maximum percentage conductivity changes in each segment of the images from the normals are given in table 1. The amount of decrease in lung conductivity with ventilation is higher in the anterior and the interior segments than in the posterior segments. The conductivity change at TLC in the lower intercostal levels is larger than the upper intercostal levels. The conductivity of the lungs decreases with forced inspiration ranging from 10% for the posterior segments of the second intercostal space up to 49% for the anterior segments of the sixth intercostal space, as the lungs are filled with air.

The images obtained at TLC are then normalized with the TLC of each subject. The TLC of the 15 normal subjects ranges between 4 and 5.5 litres with a mean of 4.9 litres. A normal mean image is obtained at each intercostal space level by averaging the corresponding pixel values of the normalized images from 15 normal subjects. These normal mean and normal

Table 1. The mean and the standard deviation of the maximum percentage conductivity changes (at TLC) in each segment of the images from the group of normal subjects, at different intercostal levels. TLC of the normal subjects ranges between 4 and 5.5 litres with a mean of 4.9 litres. Percentage conductivity changes given in the table are before normalization.

Intercostal level	RP (%)	RI (%)	RA (%)	LP (%)	LI (%)	LA (%)
Second	12 ± 7.5	32 ± 11.7	45 ± 9.6	11 ± 6.8	28 ± 13.8	47 ± 10.1
Fourth	23 ± 11.4	45 ± 12.6	45 ± 8.8	22 ± 7.5	45 ± 14.5	47 ± 9.4
Sixth	40 ± 12.9	50 ± 8.5	44 ± 11.4	38 ± 10.7	48 ± 16.4	48 ± 18

standard deviation images are shown in figure 2. In these images, higher (positive) numbers on the contours (towards blue and magenta in the colour scale) mark highly ventilated regions. At the level of the second intercostal space, only the anterior and the interior segments appear as highly ventilated regions. At lower intercostal levels the inspired air is distributed including the posterior segments. In the EIT images of the levels of fourth and sixth intercostal spaces, regions of increased conductivity outlined by the contours labelled with negative numbers (towards yellow and orange in the colour scale) are observed in the centre of the images. The authors believe that these regions may correspond to the mediastinum being pushed into a highly resistive tissue region as a result of inspiration.

4. Results on the group of patients with emphysema

Emphysema is defined as 'a condition of the lung characterised by abnormal permanent enlargement of airspaces distal to the terminal bronchiole, accompanied by destruction of their walls, and without obvious fibrosis' (Snider *et al* 1985). This condition is found pathologically by the presence of non-uniform enlargement of the respiratory airspaces or by the presence of abnormal holes in the lung parenchyma. The diagnosis of emphysema is done based on clinical examinations, PFT, chest radiograms, and conventional CT images of the thorax. Conventional CT has been shown to be more sensitive than the chest radiograph in detecting emphysematous parenchyma (Bergin *et al* 1986). CT allows the quantitative assessment of emphysema, eliminating the problems with the visual assessment, hence reducing the considerable interobserver and intraobserver variability (Müller *et al* 1988).

In the EIT images, the ventilation defects in emphysematous parenchyma are observable as non-uniform changes in tissue impedance over the affected segment of the lung. The regions with emphysematous bulla demonstrate little or no conductivity change in the images, since little or no air will move into the bulla, even at forced inspiration.

As an objective analysis, a statistical confidence test is applied to outline the differences between the patient's images and the normal mean images, as explained in section 2.3. In the images of the confidence test, regions of the lungs with emphysematous bulla formations appear as positive deviations from the normal mean images (i.e. $\mu_i - p_i$ is positive). This is due to the fact that inspired air cannot enter the regions with bulla formation. Any obstruction in airways or air spaces (as in the case of COPD or some tumours) should also result in the same type of image structure. In the test images the regions with emphysematous parencyhma appear as negative values (i.e. $\mu_i - p_i$ is negative). In the emphysematous parenchyma, as a result of destruction in the walls of the alveoli several alveoli merge together forming large air spaces. These large holes in the lungs results in higher conductivity changes with inspiration, in comparison to the same number of normal alveoli filled with air. Therefore, these regions should appear in the test images as negative regions since changes higher than the normal mean images would occur in the abnormal regions.

The maximum conductivity changes in each segment of the EIT images, prior to the normalization, the TLCs, and the ages of the patients are given in table 2. The results of visual examination of the images and the results of the statistical confidence test are discussed below, for each patient. In addition, CT images and/or the EIT images of the selected cases are also given together with their confidence test results.

Patient No 1. This patient is diagnosed with emphysema and COPD. In the apex of the right lung, a large emphysematous bulla formation is observable in the CT image. In the other regions of both lungs, wide emphysematous regions are detected. On this patient, EIT
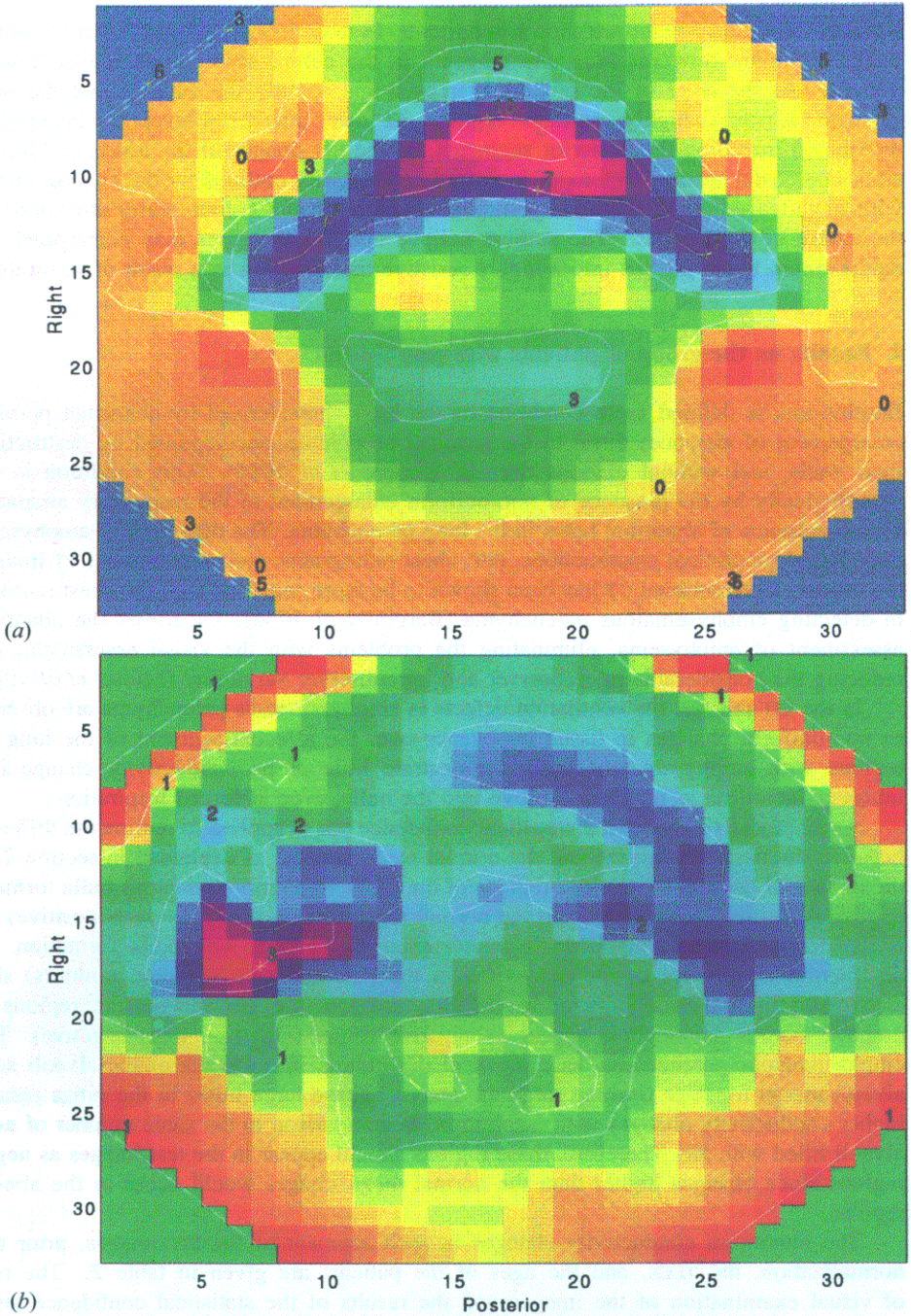
Figure 2. The normal mean and the standard deviation images of the EIT scans from 15 normal subjects. (a) The normal mean image at the second intercostal space level, (b) the standard deviation image at the second intercostal space level, (c) the normal mean image at the fourth intercostal space level, (d) the standard deviation image at the fourth intercostal space level, (e) the normal mean image at the sixth intercostal space level, (f) the standard deviation image at the sixth intercostal space level. Anterior is on the top and left is on the right.
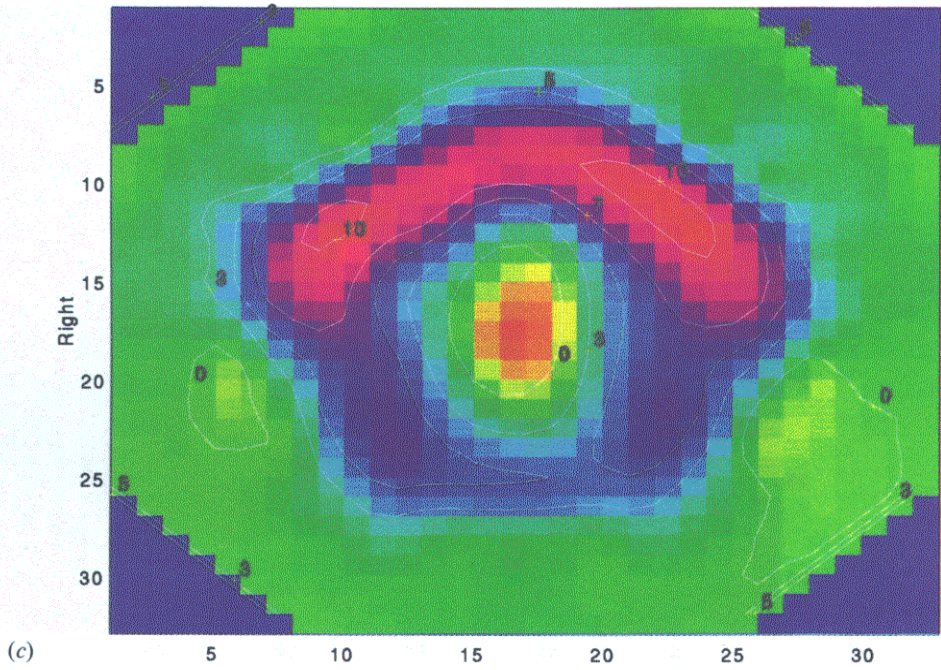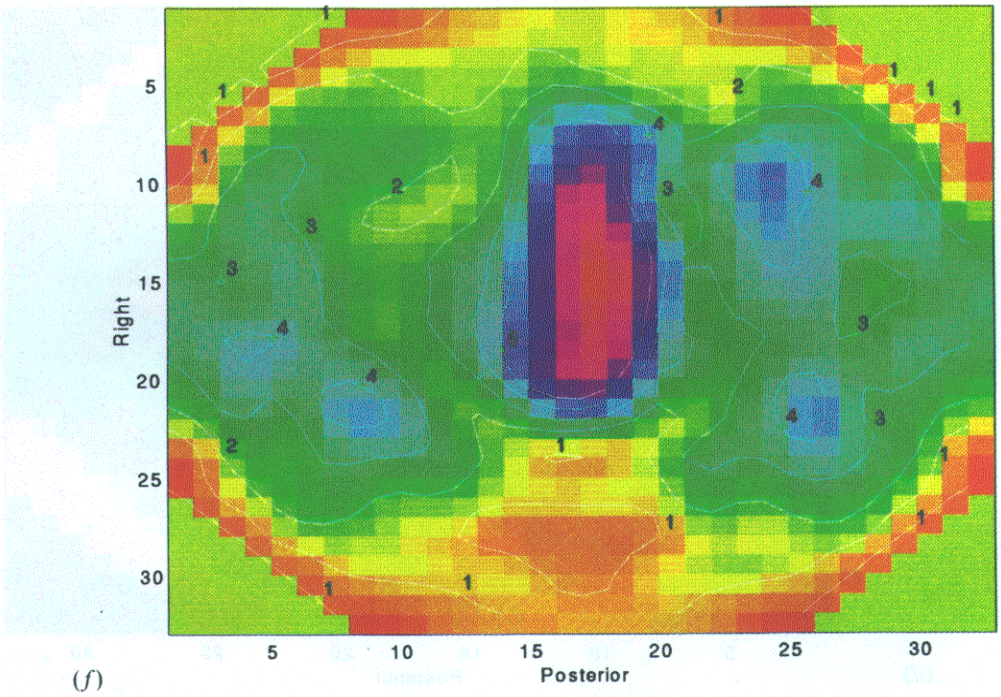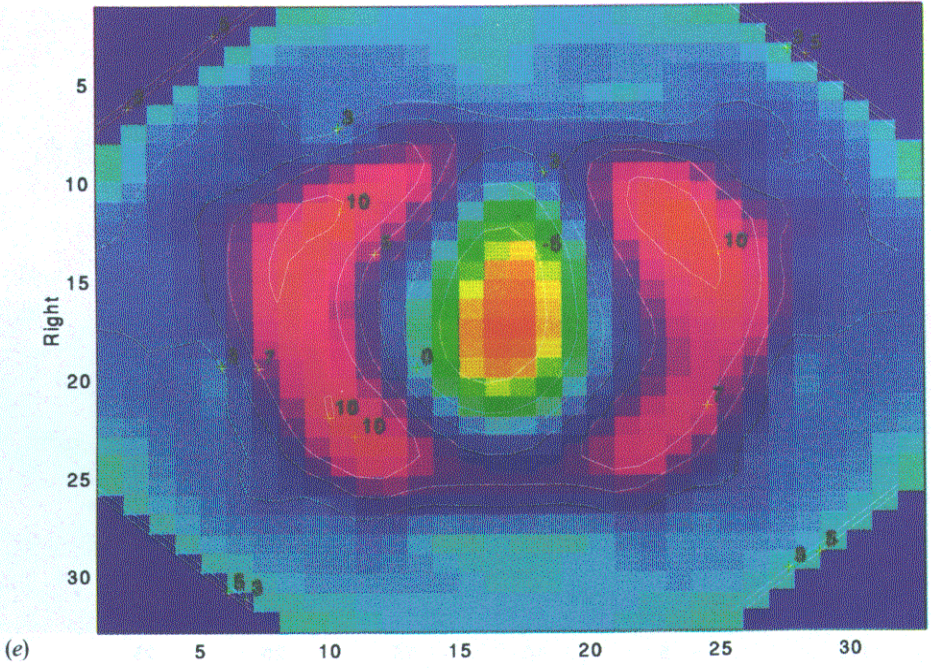
(c)
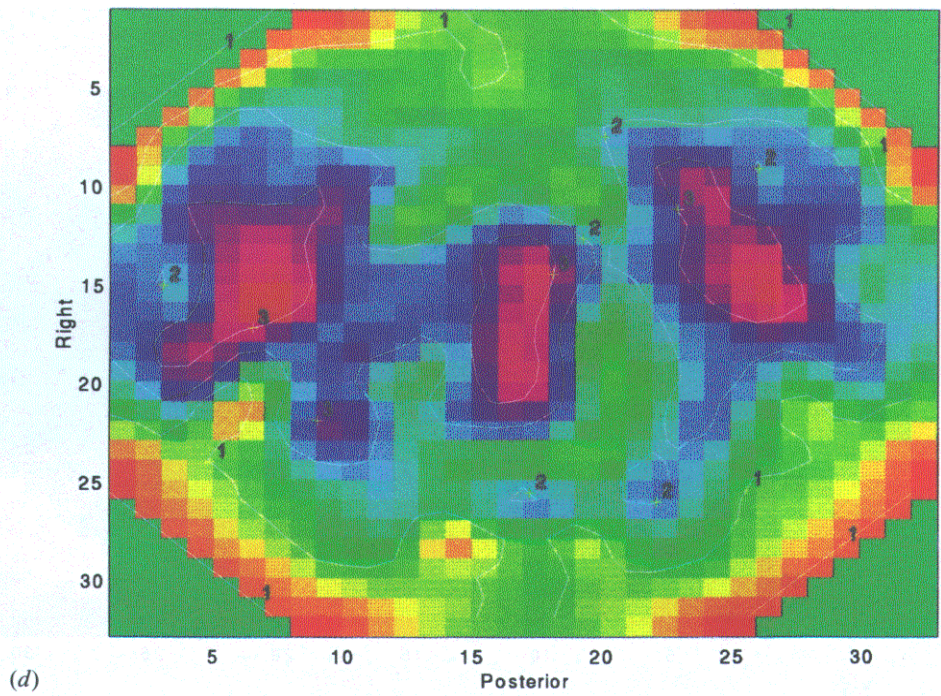
(d)

Figure 2. (Continued)

(e)

(f)

Figure 2. (Continued)

Table 2. The maximum percentage conductivity changes in each segment of the EIT images at different intercostal levels, total lung capacities (TLCs) and the ages of the patients. Percentage conductivity changes given in the table are before normalization.

Patient	Intercostal level	RP(%)	RI(%)	RA(%)	LP(%)	LI(%)	LA(%)	TLC (l)	Age
1	Second	·						2.0	65
1	Fourth	10	15	20	0	10	20	2.0	65
1	Sixth	10	20	20	0	20	20	2.0	65
2	Second	10	50	20	20	60	20	2.5	57
2	Fourth	20	20	40	20	50	40	2.5	57
2	Sixth	10	20	10	10	20	20	2.5	57
3	Second	0	20	0	0	20	0	1.5	64
3	Fourth	0	0	0	0	20	10	1.5	64
3	Sixth	0	10	0	20	40	20	1.5	64
4	Second	5	10	20	5	5	10	0.7	56
4	Fourth	10	10	40	0	5	5	0.7	56
4	Sixth	5	20	20	10	10	15	0.7	56
5	Second	0	10	0	0	10	0	1.0	55
5	Fourth	0	10	0	10	10	5	1.0	55
5	Sixth	0	15	15	0	10	15	1.0	55
6	Second	0	0	5	0	5	5	2.5	60
6	Fourth	20	20	20	10	10	10	2.5	60
6	Sixth	10	20	20	20	10	20	2.5	60
7	Second	0	5	15	0	10	20	1.2	70
7	Fourth	0	5	5	5	10	10	1.2	70
7	Sixth	0	10	5	0	10	15	1.2	70
8	Second	5	5	10	5	5	10	2.1	70
8	Fourth	10	10	5	10	10	10	2.1	70
8	Sixth	10	10	5	5	5	0	2.1	70
9	Second	0	15	0	0	5	0	1.5	51
9	Fourth	5	10	5	5	10	5	1.5	51
9	Sixth	5	10	5	0	10	5	1.5	51
10	Second	0	5	0	0	10	0	1.5	
10	Fourth								
10	Sixth	5	5	5	10	20	10	1.5	
11	Second	0	20	5	0	20	5	2.0	54
11	Fourth	0	5	0	0	5	0	2.0	54
11	Sixth	10	20	10	10	20	20	2.0	54
12	Second	5	10	20	5	10	20	1.5	61
12	Fourth	0	5	10	5	5	10	1.5	61
12	Sixth	0	5	10	0	5	20	1.5	61

images at the second intercostal space level could not be acquired since this patient had difficulty in holding his breath. Therefore, only fourth and sixth intercostal spaces were studied. The effect of emphysematous bulla is observable in the EIT images acquired at

the fourth and sixth intercostal space level. At the fourth intercostal space level, poorly ventilated regions are detected in LA, LI, LP, RP, and RI segments of the 95% confidence test image. These regions correspond to the regions with emphysematous bulla formation in the CT scans. Quantitative values before normalization corresponding to the LI and LP regions (table 2) at the sixth intercostal space level demonstrate lower values than the normals (table 1). However, when one normalizes the values for LI given in table 1 and table 2, these abnormality regions are not seen as abnormal in contradiction with the CT scans. In the test image of the sixth intercostal space level small regions with positive numbers are observed due to bulla formations in the LI, LP segments in agreement with the CT scans.
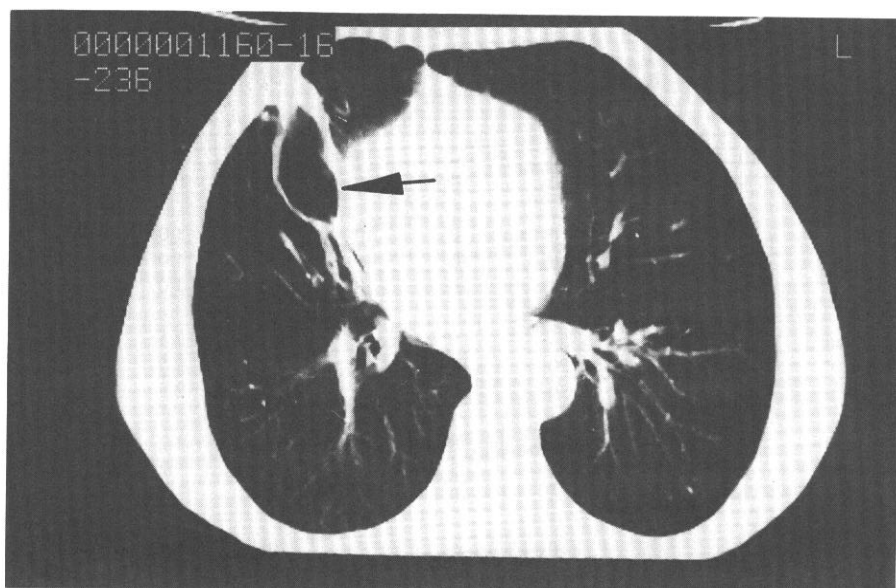
Figure 3. CT image of patient No 2 at the level of the sixth intercostal space. An emphysematous bulla with a thick wall, marked with an arrow, is located in the RA segment. Emphysematous parenchyma is observable in almost all segments, as dark black regions. Anterior is on the top and left is on the right.

Patient No 2. PFT results of this patient suggest the possibility of emphysema; however, CT images do not demonstrate emphysema at the levels of second and fourth intercostal spaces. An emphysematous bulla, with a thick wall, is observable in the RA segment of the CT images at the sixth intercostal space (figure 3). Emphysematous parencyhma is observable in all the segments of the CT image of the sixth intercostal space, as dark black regions, especially on the peripheral regions. Figure 4 shows the EIT scan at this level and the confidence test image. Although RP, RA, and LP segments have lower values (table 2), after normalization abnormal regions cannot be seen clearly in the EIT images. However, the confidence test image (figure 4(b)) shows negative deviations from the normal mean (yellow and orange in the colour scale) representing widely spread emphysematous parenchyma. The bulla with a thick wall in the RA segment cannot be distiguished in the confidence test image. This may be due to off-plane contribution of a higher conductivity change from the fourth intercostal space level RA segment (table 2) since EIT is sensitive to a volume slice rather than a thin slice.
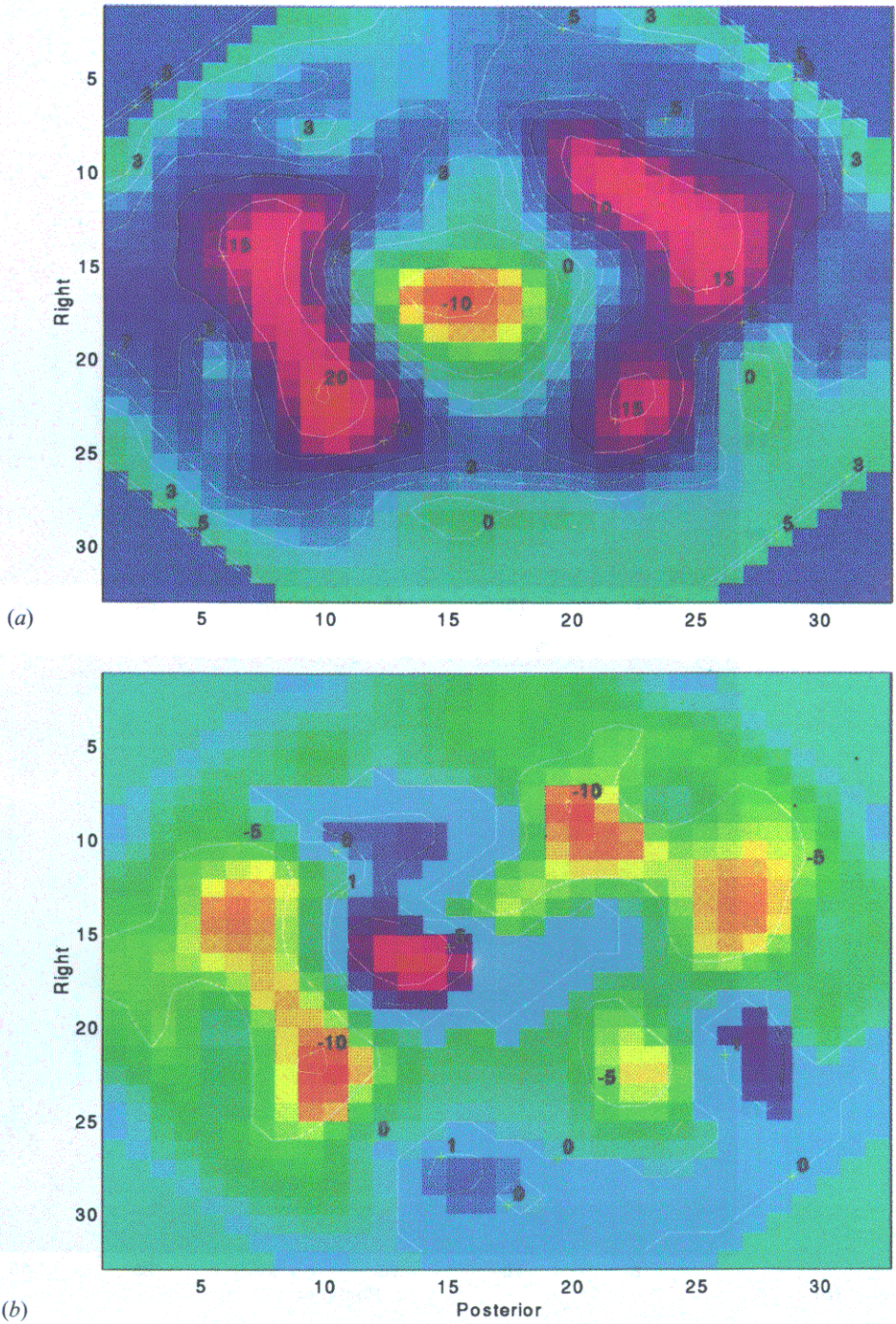
(a)

(b)

Figure 4. The normalized EIT image (a) and the confidence test image (b) obtained from patient No 2 at the sixth intercostal space level. Anterior is on the top and left is on the right.
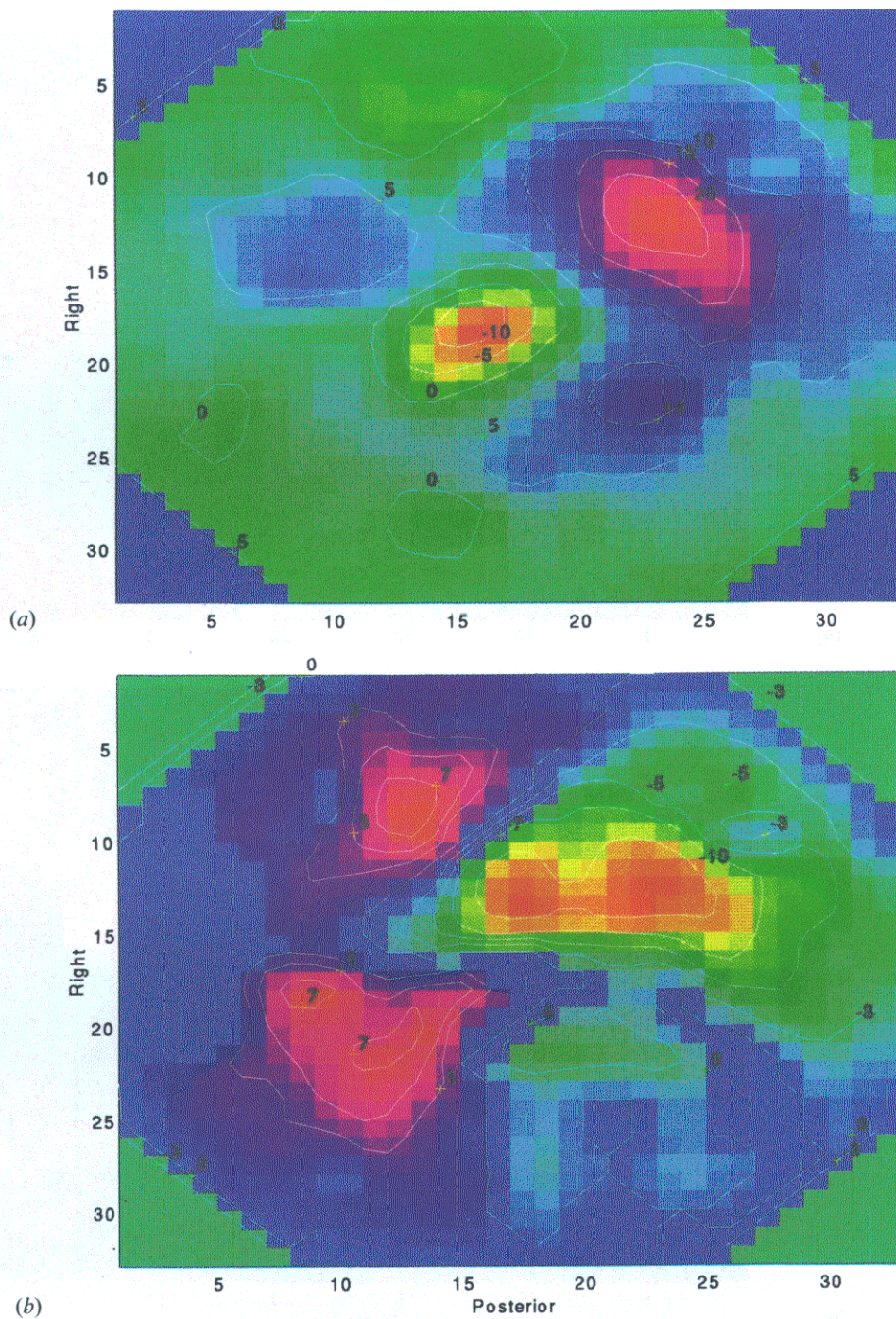
Figure 5. The normalized EIT image (a) and the confidence test image (b) obtained from patient No 3 at the sixth intercostal space level. Anterior is on the top and left is on the right.

Patient No 3. On the CT images, bilateral emphysematous bulla formations are visible in the upper lobe posterior segments. Significant volume loss of the right lung is visible. In the other parts of both lungs, emphysematous bullas spread widely. In the sixth intercostal space level emphysematous bulla formations in the RA and RP segments are observed; in the LA segment a large region of emphysematous parenchyma is detected. In the EIT images, the demonstrated as zero conductivity change in almost all the segments (table 2). The effect of the emphysematous bulla region in the LP segments of the second and fourth intercostal space levels and in the all segments of the right lung is detectable as zero-conductivity-change regions, even before normalization (table 2). The normalized EIT image at the sixth intercostal space and the corresponding confidence test image are given in figure 5. Poorly ventilated regions in the right lung are easily observable in figure 5(a). However, the emphysematous parenchyma region is not differentiable in this image, while the confidence test image of figure 5(b) demonstrates negative deviations from the normal mean in the LA segment, corresponding to emphysematous parencyhma. Bulla formations in the RA and RP segments appear clearly as positive deviations in the confidence test image. On this subject, EIT findings are in agreement with the CT images.
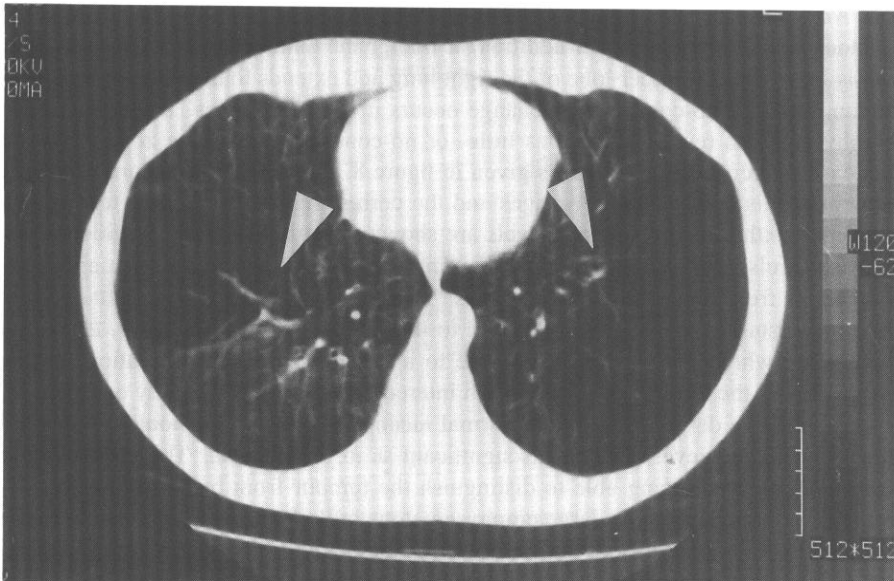

Figure 6. The CT image of the sixth intercostal space level of patient No 4. Regions of emphysematous bulla formation (dark black regions) are marked with arrows. Anterior is on the top and left is on the right.

Patient No 4. Based on the CT images, this patient has emphysematous bulla formations and parenchyma widely spread in both lungs, being most significant in the fourth intercostal space level of the left lung. In the CT images emphysematous bulla in the RP segment and in the left lung are detected at the second intercostal space level. In the fourth intercostal space there are bulla formations in the left lung and a small bulla formation in the RI segment. The CT image of the sixth intercostal space level of the same subject is given in figure 6. At this intercostal space level, emphysematous parenchyma in anterior segments are detected.

There is a bulla formation in the RI segment and in the left lung a bulla formation is seen behind the heart. Regions of emphysematous bulla formations and parenchyma (dark black regions) are marked with arrows in this image. The EIT image and the confidence test image of this patient at the sixth intercostal level are given in figure 7. In the confidence test image, the emphysematous parenchyma regions appear as negative deviations (yellow and orange in the colour scale) and bulla regions as positive deviations (dark blue and magenta in the colour scale) from the normal mean. The EIT image and the confidence test image clearly demonstrate the abnormalities in different segments.

Patient No 5. Bilateral emphysematous parenchyma and bullas are observable in the CT images, being more significant on the apex of the right lung. Quantitative changes reconstructed in the EIT images are in agreement with the findings of the CT images. Zero conductivity change is obtained in the regions where emphysematous bullas are located (table 2). Although the large bulla formations appear as zero conductivity change in EIT images (table 2), the emphysematous parenchyma and the bulla formations are not distinguishable from each other with visual only analysis. They both appear as poorly ventilated regions compare to the unnormalized normal images. Confidence test images demonstrate positive and negative deviations from the mean image at the regions where bulla formations and emphysematous parenchyma are located, respectively.

Patient No 6. The CT image of this patient displays widely spread bilateral emphysematous bulla formations. In addition, a malignant tumour structure is observed. The tumour is located in the upper lobe of the right lung and extends to the lower part. In the tumour region, little- or no-conductivity-change occurs in the EIT images. Both the tumour and the emphysematous regions appear as little- or no-conductivity-change zones. The CT scan of the sixth intercostal space level is given in figure 8. The tumour structure is seen in the RP segment at this level. The EIT images and the corresponding confidence test images of the fourth and sixth intercostal space levels are shown in figure 9. In the confidence test images at these levels, bulla formations and the tumour regions of no ventilation appear as positive deviations from the normal mean images. The positive deviation in the RP segment of the sixth intercostal space should correspond to the tumour region. However, EIT is not able to distinguish whether this deviation is due to a tumour or a bulla formation. In the posterior segments of the test image of the fourth intercostal space level, mainly on the right, there is a small positive deviation from the normal mean. This deviation should correspond to the tumour region; however, it is not as significant as in the CT scan. The major failure of EIT in this patient is not being able to distinguish the tumour from bulla formation.

Patient No 7. In the CT images, large emphysematous bulla formations are visible in the posterior regions of the apex of both lungs. Emphysematous bulla formations are observed in RP and LP segments of the fourth and sixth intercostal space levels. Emphysematous parenchyma is detectable in the anterior and posterior peripheral regions of the left lung. In the EIT confidence test images, these pathologies are marked as positive deviations from the normal mean in the case of bulla formations and as negative deviations from the normal mean as if there is an emphysematous parencyhma. Overall, EIT images are in agreement with the CT images.

Patient No 8. This patient does not have emphysema based on his CT images. He is diagnosed with COPD. As a result of the obstruction in the airways EIT images show low conductivity change in all the segments of each level (table 2). However, it is not possible to distinguish between COPD and emphysema on the EIT images. All poorly ventilated regions appear as positive deviations from the normal mean as in the case of bulla formations. In the RP segments of the second and fourth intercostal space levels confidence test images demonstrate negative deviations from the normal mean as if there is an emphysematous
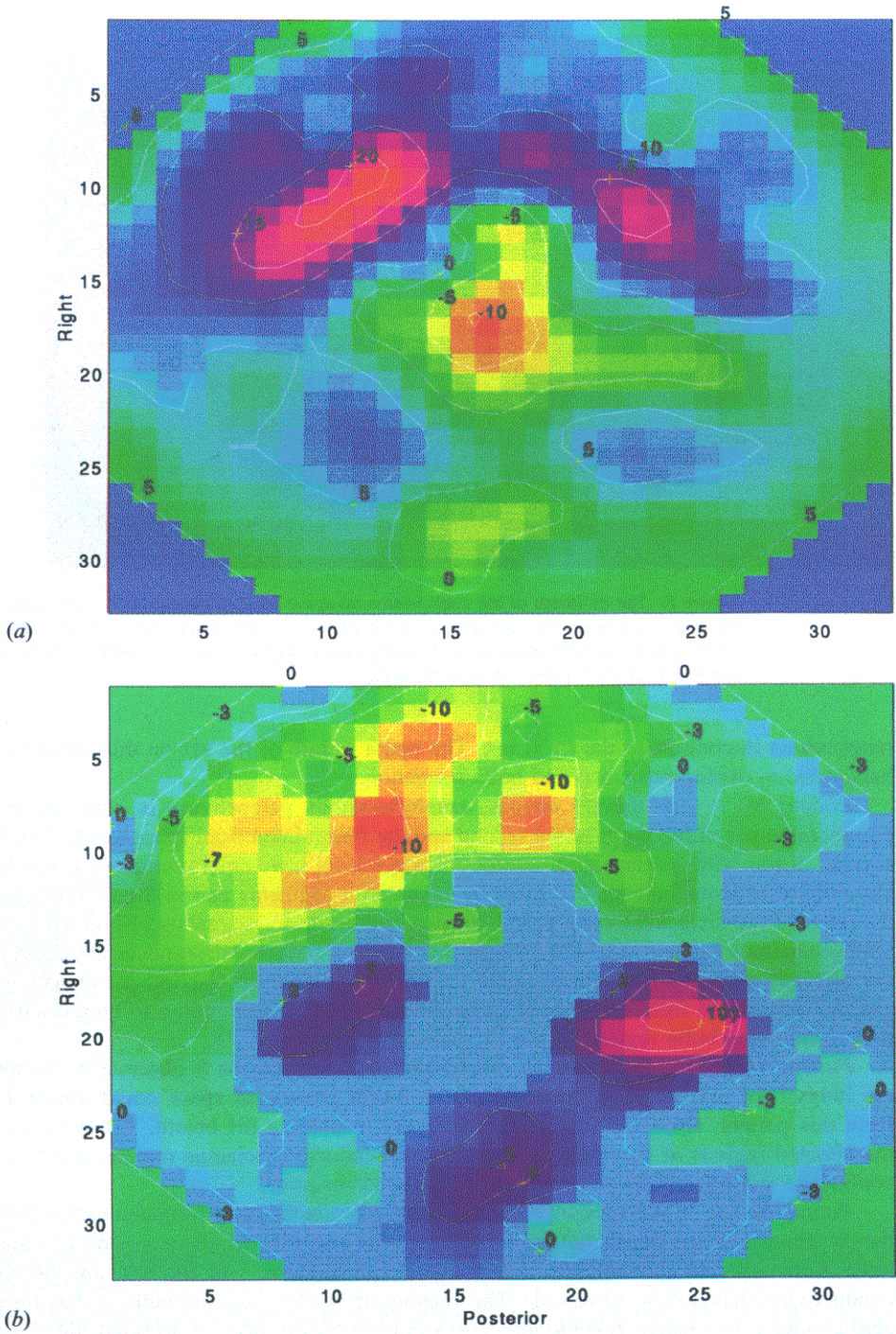
Figure 7. The normalized EIT image (a) and the confidence test image (b) obtained from patient No 4 at the sixth intercostal space level. Anterior is on the top and left is on the right.
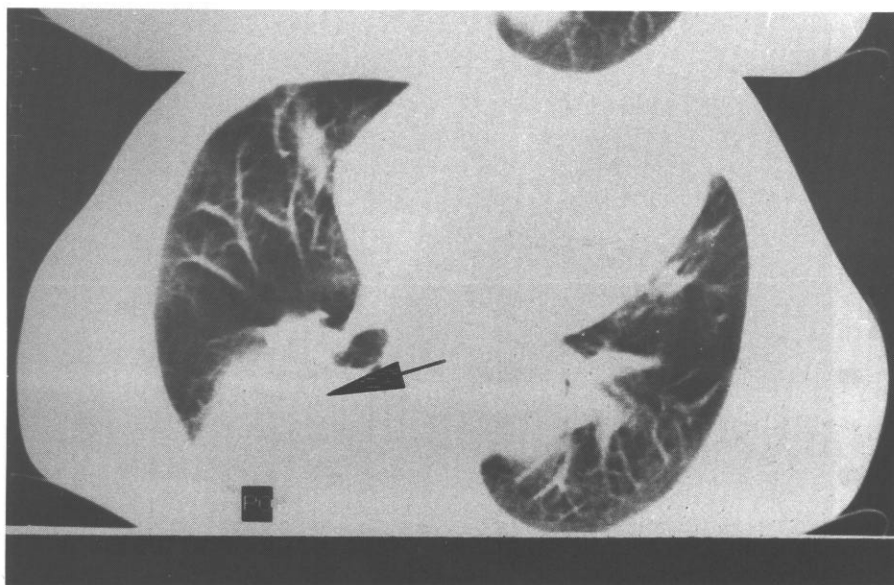
Figure 8. The CT image of the sixth intercostal space level of patient No 6. This patient has bilateral emphysematous parenchyma which appears as dark black regions in the image. A malignant tumour structure is located in the posterior segment which is marked with the arrow. Anterior is on the top and left is on the right.

parencyhma in contrast to the CT scans. The major failure of the EIT on this subject is not being able to distinguish COPD and bulla formation.

Patient No 9. In the CT images, emphysematous parenchyma is observed in the peripheral zones of the lungs at the second and the fourth intercostal space level. Peripheral regions of the lungs at the fourth intercostal space level have emphysematous parenchyma and emphysematous bullas are located in the anterior segments and in the LP segment. At the level of the sixth intercostal space, anterior and posterior segments of both lungs have emphysematous bullas. The EIT images demonstrate little or no conductivity change in the affected regions of the lungs (table 2). In the confidence test images, negative and positive deviations from the normal mean are observed corresponding to emphysematous parencyhma and bulla regions of the CT scans, respectively.

Patient No 10. In the CT images, emphysematous parenchyma is observable throughout the lungs. An EIT image at the level of the fourth intercostal space could not be taken from this patient, since the subject had difficulty in holding his breath. EIT images show the affected regions of the lungs as low- or zero-conductivity-change regions (table 2). EIT confidence test images are in agreement with the CT images.

Patient No 11. In the apex of both lungs emphysematous bulla formations are visible in the CT images. At the fourth and the sixth intercostal space levels, there are emphysematous bulla formations in the anterior and the posterior regions. In the EIT images, small conductivity changes are observed. The regions of emphysematous bulla are outlined as zero-conductivity-change zones (table 2). Overall, EIT confidence test images demonstrate the abnormal zones in agreement with the CT images.

Patient No 12. Widely spread emphysematous parenchyma and bulla formations are observed in the CT images of this patient. The defect is more significant in RP and LP

segments. EIT images show zero-conductivity-change for these highly affected regions and values lower than the normals for the other segments, indicating the existence of the ventilation abnormality (table 2). EIT confidence test images are in agreement with the CT images.

5. Problems in the clinical environment

The authors would like to summarize the problems which have been come across during the data collection from patients. Placement of electrodes and maintaining reliable electrode contacts are one of the major difficulties in the clinical environment. A more practical way of applying electrodes needs to be developed. Use of a belt electrode array (McAdams *et al* 1994) may be a significant improvement in this respect.

Patients with respiratory disorder have difficulty in holding their breath. Therefore, reducing the breath hold periods during data acquisition may be significant relief for these subjects. Filtering instead of temporal averaging should be used to eliminate cardiac-related impedance changes as implemented by Leathard *et al* (1994).

6. Discussion and conclusion

EIT ventilation images from a group of 12 patients and 15 normal subjects at the levels of second, fourth, and sixth intercostal spaces are acquired. Eleven of the patients are diagnosed with emphysema, one patient is diagnosed as having only COPD, based on their clinical examination, PFT, and CT images of the thorax, prior to the study. One of the patients with emphysema has also a malignant tumour in his right lung. The EIT images of the patients are compared with the CT scans and the quantitative changes in lung resistivity of the patients are compared with those of the group of normal subjects both visually and by applying a statistical confidence test.

For almost all the patients, EIT images are able to locate the obstruction of air flow as marked differences in conductivity changes from the group of normal subjects as a result of visual examination. In the EIT images, the ventilation defects in emphysematous parenchyma are observable as non-uniform changes in tissue impedance higher than the normal, over the affected segment of the lung. The regions with emphysematous bulla demonstrate little or no change in the images, since little or no air will penetrate into the bulla, even at TLC. In the regions of emphysematous parenchyma the changes are less than the normals. Conductivity changes in the affected segments of the lungs are less than 20% while the mean change in the group of normal subjects can be as high as 47% at TLC with respect to residual volume. The normal group is not age matched with the patient group and the TLC of the normals is at least twice as much as (in some cases almost five times larger than) the TLC of the patients. It is possible that some of the differences in the patient group might be attributable to these differences. Therefore, prior to statistical analysis all images are normalized with TLC to minimize the effect of mismatch between the ages and the TLCs of different subjects. A normal mean image is created by averaging the images from the normal subjects at each intercostal space level. Than a 95% confidence interval is defined for the normal mean. For each image of the patients a confidence test image, representing the deviations from the 95% confidence interval of the normal mean image, is created. After normalizing the normal images and the patient images with TLCs, it is observed that emphysematous parenchyma regions do not appear as regions with lower conductivity changes than normal any more. In
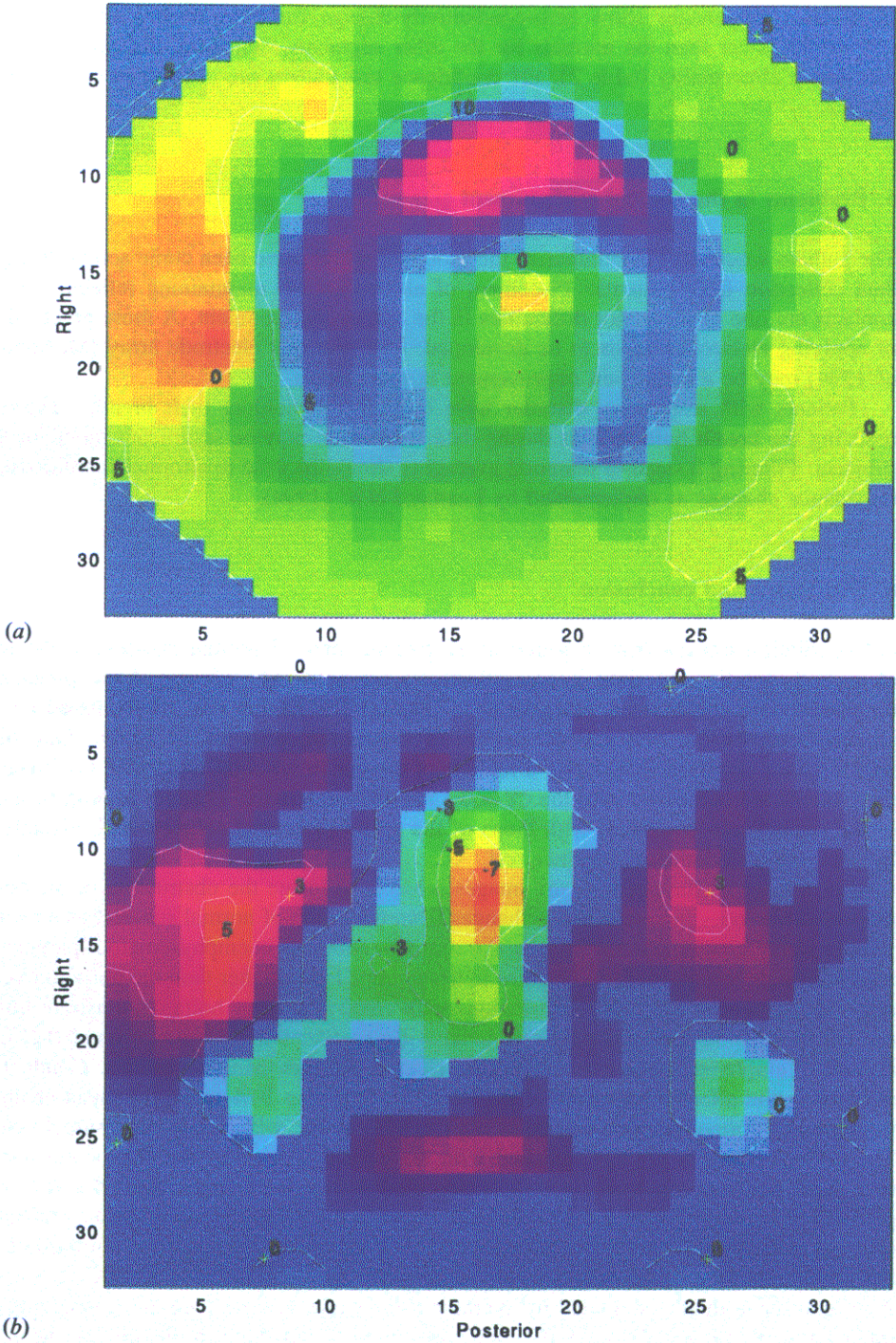
(a)

(b)

Figure 9. Normalized EIT images and confidence test images of patient No 6. (a) The EIT image at the fourth intercostal space level, (b) the confidence test image at the fourth intercostal space level, (c) the EIT image at the sixth intercostal space level, (d) the confidence test image at the sixth intercostal space level. Anterior is on the top and left is on the right.
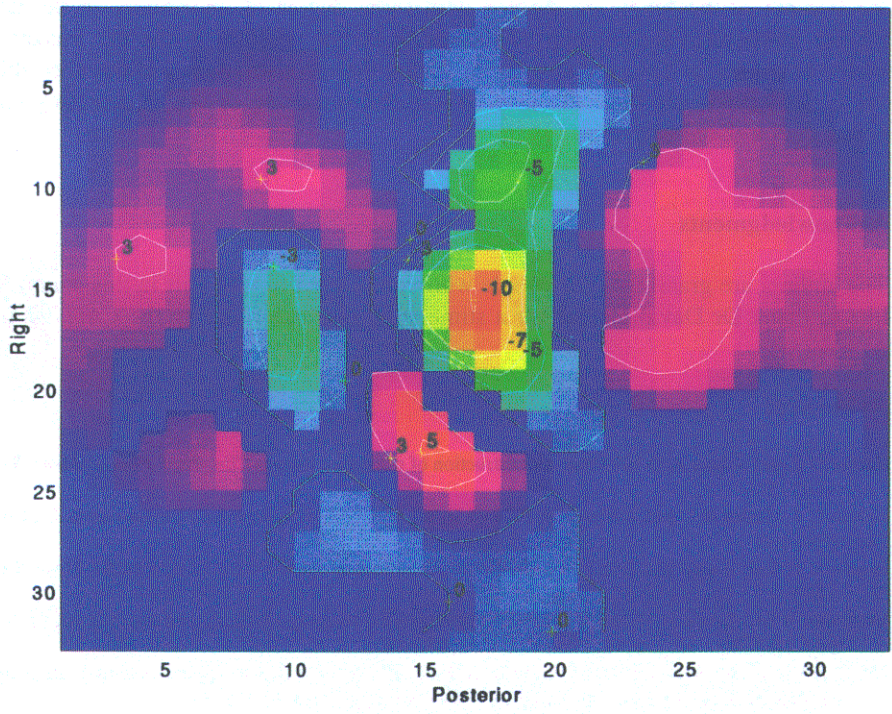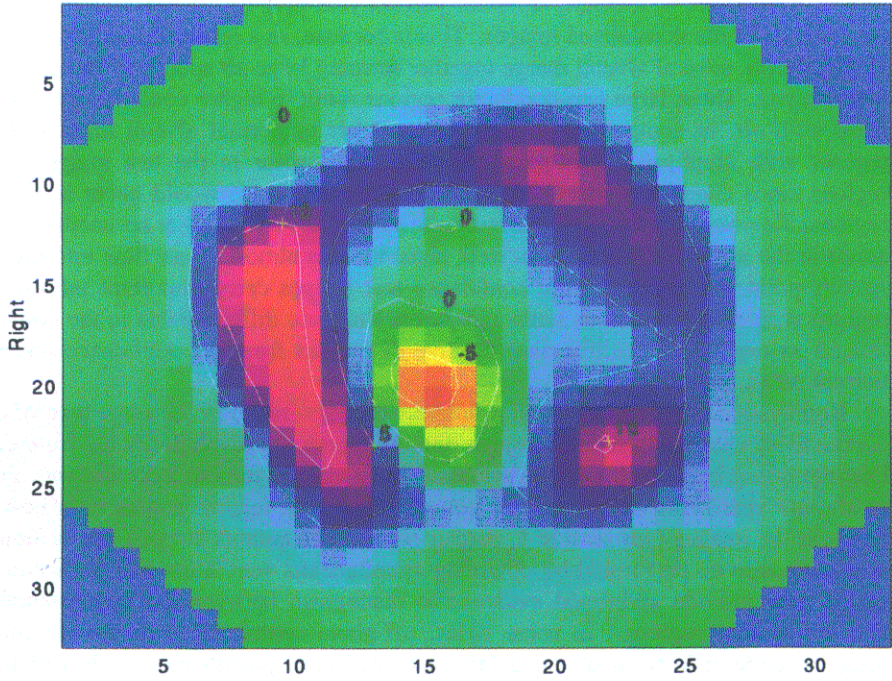
(c)

(d)

Figure 9. (Continued)

fact, those regions with emphysematous parenchyma give higher conductivity changes than the normals in the normalized images. This is because, as a result of destruction in the walls of the alveoli, several alveoli merge together forming large air spaces in the emphysematous parenchyma. These large non-conductor regions result in higher conductivity changes when filled with air, in comparison to the same number of normal alveoli filled with air. The regions with emphysematous parencyhma should appear in the test images as negative regions since changes higher than the normal mean images would occur in the abnormal regions. Regions with emphysematous bulla appear as very-little- or no-conductivity-change zones in the normalized images as well, since there is almost no air flow into these regions. At this point, the results of the confidence test images carry important information. The regions with emphysematous bulla and parencyhma are differentiable in the confidence test images as regions of positive and negative deviations from the confidence interval of the normal mean, respectively.

Emphysematous bulla, tumour structure, and COPD result in the same type of defect (no conductivity change) in the test images and are therefore indistinguishable from each other. Distinguishing between the emphysematous bulla and the tumour structure was not possible on the EIT ventilation images of one patient, since both regions appeared as no-ventilation zones in the images (see section 4, patient No 6). The authors suggest that a future clinical study needs to be performed by obtaining simultaneous ventilation and perfusion EIT scans which may provide additional evidence to distinguish between the emphysematous bulla and the tumour regions. In some cases, off-plane contributions in the EIT images may result in underestimation of the defect (see section 4, patient No 2). It will be difficult to detect small regions of abnormality, especially if they are located peripherally, since the borders of the lungs are defined with some degree of uncertainty in the EIT images. Precise anatomical localization of the lesion is not possible in the EIT images since the image boundary is distorted to a circle during the reconstruction and the slice thickness of EIT is not sufficiently thin. EIT may be a useful screening device in detecting emphysema rather than a diagnostic tool.

Acknowledgments

References

Barber D C and Seagar A D 1987 Fast reconstruction of resistance images *Clin. Phys. Physiol. Meas.* **8** (Supplement A) 47–54

Bergin C J, Müller N L and Miller R R 1986 CT in the quantitative assessment of emphysema *J. Thorac. Imaging* **1** 94–103

Brown B H and Seagar A D 1987 The Sheffield data collection system *Clin. Phys. Physiol. Meas.* **8** (Supplement A) 91–7

Eyüboğlu B M, Brown B H and Barber D C 1989 *In-vivo* imaging of cardiac-related impedance changes *IEEE Eng. Med. Biol. Mag.* **8** 39–45

Harris N D, Suggett A J, Barber D C and Brown B H 1987 Applications of applied potential tomography (APT) in respiratory medicine *Clin. Phys. Physiol. Meas.* **8** (Supplement A) 155–65

—— 1988 Applied potential tomography: a new technique for monitoring pulmonary function *Clin. Phys. Physiol. Meas.* **9** (Supplement A) 79–85

Hines W W and Montgomery D C 1990 *Probability and Statistics in Engineering and Management Science* (New York: Wiley) p 752

Holder D S and Temple A J 1993 Effectiveness of the Sheffield EIT system in distinguishing patients with pulmonary pathology from a series of normal subjects *Clinical and Physiological Applications of EIT* ed D S Holder (London: UCL Press) pp 277–98

Leathard A D, Brown B H, Campbell J, Zhang F, Morice A H and Tayler D 1994 A comparison of ventilatory and cardiac-related changes in EIT images of normal human lungs and of lungs with pulmonary emboli *Physiol. Meas.* 15 (Supplement A) A137–A146

McAdams E T, McLaughlin J A and Anderson J M 1994 Multi-electrode systems for electrical impedance tomography *Physiol. Meas.* 15 (Supplement A) A101–A106

McArdle F J, Suggett A J, Brown B H and Barber D C 1988 An assessment of dynamic images by applied potential tomography for monitoring pulmonary perfusion *Clin. Phys. Physiol. Meas.* 9 (Supplement A) 87–91

Müller N L, Stables C A, Miller R R and Abboud R T 1988 Density mask. An objective method to quantitate emphysema using computed tomography *Chest* 4 782–7

Snider G L, Kleinerman J, Thurlbeck W M and Bengali Z H 1985 The definition of emphysema. Report of a National Heart, Lung and Blood Institute, Division of Lung Diseases Workshop *Am. Rev. Respir. Dis.* 132 182–5